



HAL
open science

Particle Pressure: A Bridge from Osmosis to Granular Dilatancy

Angélique Deboeuf, Georges Gauthier, Jérôme Martin, Yevgeny Yurkovetsky,
Jeffrey F Morris

► **To cite this version:**

Angélique Deboeuf, Georges Gauthier, Jérôme Martin, Yevgeny Yurkovetsky, Jeffrey F Morris. Particle Pressure: A Bridge from Osmosis to Granular Dilatancy. *Physical Review Letters*, 2009, 102 (10), 10.1103/PhysRevLett.102.108301 . hal-02941621

HAL Id: hal-02941621

<https://hal.science/hal-02941621>

Submitted on 17 Sep 2020

HAL is a multi-disciplinary open access archive for the deposit and dissemination of scientific research documents, whether they are published or not. The documents may come from teaching and research institutions in France or abroad, or from public or private research centers.

L'archive ouverte pluridisciplinaire **HAL**, est destinée au dépôt et à la diffusion de documents scientifiques de niveau recherche, publiés ou non, émanant des établissements d'enseignement et de recherche français ou étrangers, des laboratoires publics ou privés.

Particle pressure: A bridge from osmosis to granular dilatancy

Angélique Deboeuf, Georges Gauthier, and Jérôme Martin
*Univ Pierre et Marie Curie-Paris6, Univ Paris-Sud, CNRS, Laboratoire FAST,
Campus universitaire d'Orsay, 91405 Orsay CEDEX, FRANCE*

Yevgeny Yurkovetsky and Jeffrey F. Morris
Levich Institute and Chemical Engineering; City College of New York; New York, NY 10031 USA
(Dated: January 8, 2009)

The normal stress exerted by particles in a sheared suspension is measured by analogy with a method used to measure osmotic pressure in solutions. Particles in a liquid of equal density are confined by a fine screen to a gap between two vertical concentric cylinders, the inner of which rotates. Pressure in the liquid is sensed either by a manometer or by a pressure transducer across the screen. The particles are large enough so that Brownian motion and equilibrium osmotic pressure are vanishingly small. The measured pressure yields the shear-induced particle pressure Π , which is the nonequilibrium continuation of equilibrium osmotic pressure. For volume fractions $0.3 \leq \phi \leq 0.5$, Π is strongly dependent on ϕ , and linear in shear rate. Comparisons of the measured particle pressure with modeling, experimental derivations, and simulation show good agreement.

Motion of one component relative to the remainder of a mixture may arise from different sources, including a density difference or concentration gradient. Driving force is often described in terms of a potential, *e.g.* the gravitational potential energy for settling particles. However, diffusion is usually accounted through a Fickian flux, $\mathbf{j} = -D\nabla n$, with D the diffusivity and n the solute number density. Because diffusion results from irregular stochastic motion, defining an associated potential is not trivial. The desired potential is, however, obtained from the relation between diffusion and osmotic pressure and this is considered as a prelude to a striking extension of osmotic pressure in flowing mixtures.

Random motion of dissolved molecules and ions, or of submicron particles, results in diffusion scaling as the thermal energy kT . In the absence of other influences, diffusion tends to drive the mixture toward the homogeneous equilibrium state with $\nabla n = \mathbf{0}$. A key development was provided by Einstein [1], who considered a dilute dispersion of particles in an external field of potential energy U . The force $\mathbf{F} = -\nabla U$, applied to each particle, induces a flux $n\mathbf{u}$ with the velocity given by $\mathbf{u} = M\mathbf{F}$ where M is the mobility of the solute particles. In the resulting inhomogeneous – but nonetheless equilibrium – state, the flux due to the external field balances the diffusive flux so that $-nM\nabla U - D\nabla n = 0$. Requiring Boltzmann distribution of energy at equilibrium, $n \sim \exp[-U/kT]$, yields both the *thermodynamic force* $\mathbf{F}_{\text{th}} = -kT\nabla \ln n$ and the celebrated result $D = kTM$. Moreover, as pointed out by Einstein, the volumetric thermodynamic force $n\mathbf{F}_{\text{th}}$ can be written as $-\nabla\Pi_{\text{osm}}$, where Π_{osm} is the osmotic pressure which obeys the van't Hoff relation for dilute systems [2], $\Pi_{\text{osm}} = nkT$. Hence, the Fickian flux may also be written $\mathbf{j} = -M\nabla\Pi_{\text{osm}}$. Diffusive flux and osmotic stress are then two complementary descriptions to account for the influence of random motion of a solute. These motions cause diffu-

sive mixing but also tend to minimize variations of the Helmholtz free energy A , leading to a thermodynamic definition of the osmotic pressure, $\Pi_{\text{osm}} = -(\frac{\partial A}{\partial V})_{N,T}$, with N the number of solute particles.

This thermodynamic approach provides a convenient means to describe osmosis, which occurs when a solution is separated from a lower concentration solution or the pure solvent by a ‘semipermeable membrane’ allowing the flow of the solvent but restricting the solute to the solution side, as in a U-tube osmometer sketched in the left of Fig. 1. In this context, Π_{osm} is the additional pressure which must be applied to the solution side to stop solvent flow, *i.e.* to reach the equilibrium state. Note that this solvent flux was first observed in 1748 [3], but its interpretation as a decrease of the free energy by dilution was proposed much later. In practice, osmotic driving forces can be large: As an example, sea water contains ions at $n \approx 1.4$ mol/L (2.5 mole %) and has $\Pi_{\text{osm}} \approx 25 - 30$ atmospheres, surprisingly large yet in line with the van't Hoff relation for dilute solutions.

Here we illustrate that unexpected osmotic phenomena occur in sheared suspensions of large particles. We recall first that for hard spheres, $\Pi_{\text{osm}} = nkT[1 + 4\phi g(2)]$ where the volume fraction is $\phi = 4\pi na^3/3$ for spheres of radius a , and $g(2)$ is the contact value of the pair distribution function [4]. Away from the divergence of g at maximum packing, *i.e.* for concentrations smaller than $\phi_{\text{max}} \approx 0.64$, this expression yields $\Pi_{\text{osm}} \sim kT/a^3$, of $O(1)$ Pa for $a = 0.1 \mu\text{m}$ and $O(10^{-3})$ Pa for $a = 1 \mu\text{m}$. For larger particles, osmotic pressure and Brownian motion are then vanishingly small, but these ‘noncolloidal’ suspensions nevertheless exhibit diffusion in sedimentation or shear [5, 6], induced by the chaotic particle trajectories [7] caused by hydrodynamic interactions.

The interactions generate ‘shear-induced diffusion’ which dissipates concentration gradients [8, 9]. Rather remarkably, particle interactions driven by a spatially

varying shear rate, $\dot{\gamma}$, can generate concentration gradients. For unidirectional flow $u_x(y)$ this implies a cross-stream particle flux $\mathbf{j} \sim -\nabla\dot{\gamma}$, where $\dot{\gamma} = |du_x/dy|$ [5]. As an alternative, a ‘particle pressure’ Π has been invoked as the driving potential for particle migration [10, 11]. Particle pressure and shear-induced diffusion are the counterparts in sheared systems of the thermal osmotic pressure and Brownian diffusion, respectively.

Our purpose is to further develop the connection, described in theory and simulation studies [12, 13], between nonequilibrium particle pressure Π and osmotic pressure. In particular, we illustrate that Π may be measured using a method directly analogous to the classical approach for the measurement of osmotic pressure. The experiments show that osmosis in mixtures is a general result of constraining the dispersed phase against spreading. This leads to the notion that Π quantifies the general tendency of a dispersed phase to spread, an idea long associated with Reynolds dilatancy [14] in which a granular assembly, with grains in contact, must expand to shear.

We turn now to the experimental method. When solute or particles are constrained from spreading, stresses arise in the mixture leading to solvent flow into the solution. Osmotic pressure, associated with the drive toward solute spreading and hence a compressive stress in the dispersed component, is thus measured as a reduced pressure in the solvent. We use this as the conceptual basis to measure the pressures induced by shear flow in the two phases of a viscous suspension. Shear-induced particle pressure has eluded direct measurement in large part because opposing stress states of solvent and dispersed phase lead to a cancellation [13, 15]. To measure Π requires, as for Π_{osm} , a method which either allows relative motion so the dispersed phase may change its concentration, or alternatively directly senses the driving force for relative motion. We describe both approaches.

We use suspensions of polystyrene spheres (Dynoseeds TS; Microbeads) of diameter 40, 80, or 140 μm ($\pm 5\%$ in each case, with AFM-measured roughness ≈ 100 nm), with density $\rho = 1.05$ $\text{g}\cdot\text{cm}^{-3}$ matching the suspending liquid. The viscosity of the Newtonian fluid, poly(ethylene glycol-ran-polypropylene glycol) monobutyl ether, is $\eta_f = 3$ Pa.s at 20°C. The bulk suspension viscosity agrees well with the form $\eta(\phi)/\eta_f = (1 - \phi/\phi_{\text{max}})^{-2}$. The ratio of shear to Brownian motion, or Péclet number, is $Pe = 6\pi\eta_f\dot{\gamma}a^3/kT = O(10^8)$ at $\dot{\gamma} = 1$ s^{-1} . Thermal motion is negligible.

The analogy of the device used here to a U-tube osmometer with semipermeable membrane is illustrated in the center sketch of Fig. 1. The actual Couette device is shown at right in Fig. 2. The inner and outer cylinders have radii $r_1 = 17.5$ mm and $r_2 = 20$ mm, respectively, leaving an annular gap $r_2 - r_1 = e = 2.5$ mm. Rotation of the inner cylinder generates a shear rate $\dot{\gamma} \approx \Omega r_1/e$. Variation of shear rate across the gap is small and we report only the average. The flow is viscous as the Reynolds

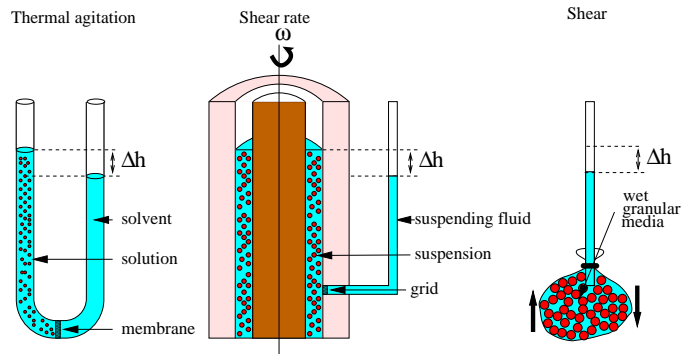


FIG. 1: Left: U-tube osmometer. Center: Schematic of the experimental apparatus. Right: Reynolds dilatancy.

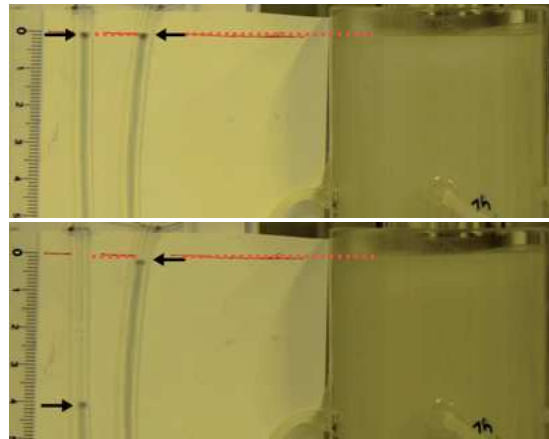


FIG. 2: Manometer approach for a suspension of 80 μm diameter particles at $\phi = 0.4$. Couette device is at right, with the upper surface of the suspension indicated by the dashed line. Meniscus levels are highlighted by arrows for screened (left tube) and open (right) holes at rest (top picture), and after 40 min of shear at $\dot{\gamma} = \Omega r_i/e = 70$ s^{-1} (bottom picture).

number is $Re = \rho\dot{\gamma}e^2/\eta_f \leq 1$. Eight holes of diameter 3 mm pass through the outer stationary cylinder. They are at 90° intervals, in two sets located 2 and 6 cm from the bottom of the sheared annulus. Screens with 20 μm square openings, small enough to retain the particles, are placed across the holes on the side toward the annulus. A tube is fixed in each hole and filled with the suspending liquid. These tubes may serve as manometers or for transmission of the liquid pressure to a transducer.

Results from the manometer approach for $\phi = 0.4$ and $\dot{\gamma} = 70$ s^{-1} are illustrated by Fig. 2. Meniscus levels are shown for a screened hole before shearing (left tube) and after forty minutes of shearing, in the top and bottom images, respectively. To demonstrate the role of the screen, the meniscus in a tube attached to an unscreened hole is also shown in Fig. 2 (right tube). Whereas the meniscus associated with the screened hole drops a few cm, the one with the unscreened hole is almost stationary, as liquid suction is balanced by solid phase dispersive pressure.

Although visually convincing and appealing for its direct analogy with the classical U-tube experiment, the manometer approach has drawbacks. The long times (hours) needed to obtain a measurement, and large Δh when ϕ and $\dot{\gamma}$ are both large render the approach inconvenient. A basic flaw is that the results are sensitive to ϕ , which is altered by the liquid drawn into the annulus. Note, however, that the manometer measurements are consistent with the approach described below.

To obtain quantitative measurements, a pressure transducer is attached to each tube. The screen is maintained, and the tubing is completely filled with the suspending liquid to provide communication between suspension and transducer. A pre-shear was applied to ensure the suspension was uniform around the annulus. The transducer reading stabilizes within a few seconds of shearing, and measurements are averaged over 1–2 minutes. No liquid is exchanged across the screen. The difference in the transducer reading between sheared and static states is ΔP , and is negative: Flow generates a suction pressure in the liquid. The pressure is averaged over forward and reverse shearing to eliminate flow-induced pressure due to any slight eccentricity of the cylinders.

Results for the suspension of 40 μm diameter particles are shown in the top panel of Fig. 3 as a function of $\eta_f \dot{\gamma}$, with the fluid viscosity η_f corrected for temperature. The measured $|\Delta P|$ is viscously-driven, as inertial effects would be greatest for the pure liquid which gives a null response, $\Delta P = 0$, and $|\Delta P|$ increases roughly linearly with increasing $\dot{\gamma}$. Note that linearity in $\dot{\gamma}$ at $Pe \gg 1$ differs from the $\dot{\gamma}^2$ dependence of normal stress observed for small Pe [16]. The magnitude increases strongly with ϕ , from $|\Delta P|/\eta_f \dot{\gamma} = 0.35$ at $\phi = 0.3$ to 18.5 at $\phi = 0.5$. Error bars are significant, but are typically small compared to the mean value. Data for the other sizes of particles studied (80 and 140 μm) are similar to the 40 μm case, although ΔP is smaller for the larger particles.

The measured suction pressures, normalized by $\eta_f \dot{\gamma}$, for all ϕ and particle sizes studied are gathered in the lower panel of Fig. 3. These show that the suction pressure measured in the liquid behaves similarly to the particle normal stress differences [11, 17]. In particular, the pressure becomes reliably measured at $\phi \approx 0.3$ and grows rapidly with ϕ . A slight radial particle migration, which can be deduced from results in [11], is complete during the pre-shear for all a , and cannot explain the difference in $|\Delta P|$ with particle size. A particle slip layer [18] will not explain the observation, although there may be a difference in organization when the gap is small ($e/2a < 20$ for the 140 μm beads) which could enhance apparent slip (as in shear banding). We note that an axial migration to, and even through, the free surface was observed and this reduces ϕ within the suspension; migration is more pronounced for larger beads. In general, these considerations lead us to expect that small particles yield the most accurate results, in accord with agreement with model

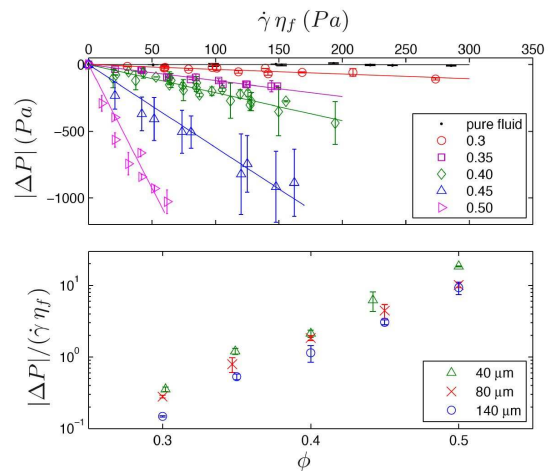


FIG. 3: Measured difference in liquid pressure between resting and sheared states, ΔP . Top: 40 μm diameter particle suspension at varying ϕ , as a function of $\eta_f \dot{\gamma}$. Error bars show the range of transducer measurements for a given condition. Bottom: $|\Delta P|/\dot{\gamma} \eta_f$ as a function of ϕ for three particle sizes.

and simulation for the 40 μm suspension (see Fig. 4).

There is a conceptual difficulty in the measurement of the particle pressure in a sheared suspension, stemming from the fact that liquid and solid both satisfy incompressibility to a close approximation. Particle pressure is thus offset by an equal and opposite change in liquid pressure [13], *i.e.* $\Pi = -\Delta P(\dot{\gamma})$. A transducer exposed to both phases measures the sum of these shear-induced stresses to yield a confusing result [15]. Hence, only a method which discriminates between the phases can enable the measurement of the particle pressure, and in our approach we make use of $\Pi = -\Delta P = |\Delta P|$. This use of the liquid pressure provides the conceptual link to osmotic pressure. The particle pressure [12] in a sheared suspension is the mean normal stress exerted by the particle phase $\Pi = -(1/3)[\Sigma_{11}^P + \Sigma_{22}^P + \Sigma_{33}^P]$ and has been shown by simulation to be equivalent to the osmotic pressure for vanishing shear rate [13], *i.e.* $\lim_{\dot{\gamma} \rightarrow 0} \Pi = \Pi_{osm}$.

However, one has to be cautious in equating the measured liquid pressure with the particle pressure, *i.e.* in using $\Pi = |\Delta P|$. The measured liquid pressure is set by the conditions at the free surface of the suspension, where deformation of the liquid surface allows capillary pressure to balance the mean particle stress in the vertical direction. It follows $|\Delta P| = \Sigma_{33}^P$, which may differ from Π . Several arguments justify the approximation $\Pi \approx |\Delta P|$. First, simulation [13] and experimental correlation [17] lead to the conclusion that normal stress differences, $N_1 = \Sigma_{11}^P - \Sigma_{22}^P$ and $N_2 = \Sigma_{22}^P - \Sigma_{33}^P$, are small relative to Π . Furthermore, the small change in the meniscus level for an unscreened hole (Fig. 2) confirms that $\Sigma_{rr}^P + \Delta P = \Sigma_{22}^P - \Sigma_{33}^P \approx 0$.

The particle pressure measured, using the approxima-

tion $\Pi = -\Delta P$, is compared in Fig. 4 with experimental correlation, simulation, and modeling. Analysis of experimental data [17] showed that migration and viscous resuspension could be rationalized by an isotropic particle stress. The resulting correlation developed for Π is plotted. The expression $\eta_n(\phi) = \Pi/\eta_f\dot{\gamma}$, from constitutive modeling for migration analysis [11] is also displayed, together with simulation values of Π at $Pe = 1000$ [13] and infinite Pe [19], obtained with weak and zero thermal motion, respectively. Both simulations use Stokesian Dynamics but differ in the treatment of Π . Despite the variation observed for the different particle sizes, our measured particle pressure is in remarkable agreement with simulation and experimental correlation.

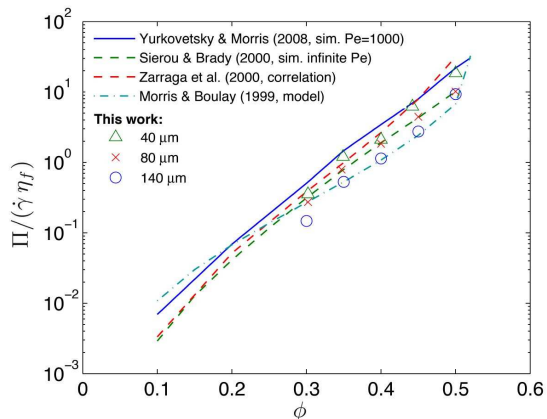


FIG. 4: Comparison of experimental correlation, simulation, and modeling of the particle pressure with the experimental values obtained in this study taking $\Delta P \equiv \Pi$.

We conclude that liquid suction pressure in a sheared suspension provides a robust means of measuring the particle pressure. The fundamental link between particle pressure and equilibrium osmotic pressure is strong. Bagnold's notion of particle pressure under shear [20] has a central role in the modeling of shear-induced migration.

The utility of $\Pi \sim \eta_f \dot{\gamma}$ for modeling is recognized and applied for noncolloidal [12, 13] and Brownian dispersions [21, 22]. Simulations have shown that the quantity agrees with equilibrium theory [13]. The present work shows direct measurability of Π , which, these models have argued, drives shear-induced migration flux [10–13]:

$$\mathbf{j} \sim \nabla \cdot \Sigma^P \approx -\nabla \Pi = - \left[\frac{\partial \Pi}{\partial \phi} \nabla \phi + \frac{\partial \Pi}{\partial \dot{\gamma}} \nabla \dot{\gamma} \right]. \quad (1)$$

Thus, particle stress can be seen to play a similar role both in and out of equilibrium. The shear-induced migration driven by $\nabla \dot{\gamma}$ generates gradients in ϕ , but nonetheless relaxes variations in Π , just as Fickian diffusion relaxes variations in Π_{osm} arising from nonzero $\nabla \phi$. One can then speculate that particle pressure pertains to a more general property of mobile particle mixtures, which

exhibit rather nonintuitive phenomena when the dispersed phase is confined. The phenomena include the well-known osmosis, observed in thermally-driven systems, and known to be related to the osmotic pressure.

Particle pressure is the nonequilibrium continuation of osmotic pressure [13] and drives shear-induced migration, known to generate inhomogeneity in pipe and channel flows [10, 23]. Because density matching is possible, Π for viscous suspensions can be explored for any ϕ , and for arbitrary ratios of shearing to thermal motion. When gravity plays a prominent role, solids loading is not freely variable. Hence, a granular medium or sediment is formed with $\phi \approx \phi_{max}$ and particles in contact. Under such conditions, shearing will induce dilation and the granular material will develop normal forces if it is sheared while constrained to the same volume. While the final link with granular dilation remains to be made, particle pressure appears to be a bridge from osmotic pressure driven by kT to the athermal mixture stresses in suspensions and granular materials.

We thank RTRA Triangle de la physique for funding, Univ. de Paris 6 for a visiting professorship (JFM), A. Aubertin and R. Pidoux for building apparatus, and D. Bonamy and G. Pallares for the AFM measurements.

-
- [1] A. Einstein, *Ann. d. Phys.* **17**, 549 (1905).
 - [2] J. van't Hoff, [hoff-lecture.pdf at nobelprize.org/](http://hoff-lecture.pdf.at.nobelprize.org/) (1901)
 - [3] J. A. Nollé, *Leçons de Physique expérimentale*, Guerin and Delatour, Paris (1748).
 - [4] W. B. Russel, D. A. Saville & W. R. Schowalter, *Colloidal Dispersions* Cambridge University Press (1989).
 - [5] D. Leighton & A. Acrivos, *J. Fluid Mech.* **177**, 109 (1987); **181**, 415 (1987).
 - [6] J. Martin, N. Rakotomalala & D. Salin, *Phys. Rev. Lett.* **74**, 1347 (1995).
 - [7] D. J. Pine *et al.*, *Nature* **438**, 997 (2005).
 - [8] V. Breedveld *et al.*, *J. Fluid Mech.* **375**, 297 (1998).
 - [9] V. Breedveld *et al.*, *J. Chem. Phys.* **116**, 10529 (2002).
 - [10] P. R. Nott & J. F. Brady, *J. Fluid Mech.*, **275**, 157 (1994).
 - [11] J. F. Morris & F. Boulay, *J. Rheol.* **43**, 1213 (1999).
 - [12] D. J. Jeffrey, J. F. Morris & J. F. Brady, *Phys. Fluids* **5**, 2317 (1993).
 - [13] Y. Yurkovetsky & J. F. Morris, *J. Rheol.* **52**, 141 (2008).
 - [14] O. B. Reynolds, *Philos. Mag.* **20**, 469 (1885).
 - [15] D. Prasad & H. K. Kytömaa, *Int. J. Multiphase Flow* **21**, 775 (1995).
 - [16] J.F. Brady & M. Vacic, *J. Rheol.*, **39** 545, (1995).
 - [17] I. E. Zarraga, D. A. Hill & D. T. Leighton, *J. Rheol.* **44**, 185–220 (2000).
 - [18] S. C. Jana, B. Kapoor & A. Acrivos, *J. Rheol.* **39**, 1123 (1995).
 - [19] A. Sierou & J. F. Brady, *J. Rheol.* **46**, 1031 (2002).
 - [20] R. A. Bagnold, *Proc. R. Soc. Lond. A* **255**, 4963 (1954).
 - [21] M. Frank *et al.*, *J. Fluid Mech.* **493**, 363 (2003).
 - [22] I. Cohen, T. G. Mason & D. A. Weitz, *Phys. Rev. Lett.* **93**, 046001 (2004).
 - [23] M. K. Lyon & L. G. Leal, *J. Fluid Mech.* **363**, 25 (1998).